Supporting Information

Roy et al. 10.1073/pnas.1009743107

SI Methods

Mice. Nck1$^{-/-}$ (1) and Nck2$^{flx/flx}$ (2) mice were crossed to Lck-Cre mice (3) (generous gift of J. Marth University of California at San Diego, La Jolla, CA). HY-TCR (4), P14-TCR (5), and RAG2$^{-/-}$ mice were kindly provided by B. Rocha (Institut National de la Santé et de la Recherche Médicale, Paris), A. Freitas (Institut Pasteur, Paris), and S. Ezine, respectively. Nck1$^{-/-}$Nck2$^{flx/flx}$*Lck*-Cre (Nck.T$^{-/-}$) mice were backcrossed to C57BL/6 mice three to four times and crossed to RAG2$^{-/-}$ HY-TCR or P14-TCR mice to obtain HY-TCR.Nck.T$^{-/-}$ and P14-TCR.Nck.T$^{-/-}$ mutant mice. Given the high number of mutations carried by each mutant strains, two types of controls were used: (*i*) *Lck*-Cre^{Ntg} Nck1$^{+/+}$Nck2$^{flx/flx}$ littermates, obtained by intercrossing Lck-Cre^{het} Nck1$^{+/-}$Nck2$^{flx/flx}$ mice; and (*ii*) *Lck*-Cre^{tg} Nck1$^{+/+}$ Nck2$^{+/+}$ mice derived from intercrosses of Lck-Cre^{tg} Nck1$^{+/-}$ Nck2$^{+/flx}$ mice. A series of experiments, in which both controls were used in parallel, enabled to control for the effects of Cre recombinase expression (6), and established the equivalence of the two strains, which are defined as Nck.T$^{+/+}$ mice throughout the article. Phenotypic and functional data have been confirmed in Nck.T$^{-/-}$ and Nck.T$^{+/+}$ lines, derived from 10 backcrosses to C57BL/6 mice.

1. Bladt F, et al. (2003) The murine Nck SH2/SH3 adaptors are important for the development of mesoderm-derived embryonic structures and for regulating the cellular actin network. *Mol Cell Biol* 23:4586–4597.
2. Jones N, et al. (2006) Nck adaptor proteins link nephrin to the actin cytoskeleton of kidney podocytes. *Nature* 440:818–823.
3. Orban PC, Chui D, Marth JD (1992) Tissue- and site-specific DNA recombination in transgenic mice. *Proc Natl Acad Sci USA* 89:6861–6865.
4. Kisielow P, Teh HS, Blüthmann H, von Boehmer H (1988) Positive selection of antigen-specific T cells in thymus by restricting MHC molecules. *Nature* 335:730–733.
5. Brändle D, et al. (1991) Involvement of both T cell receptor V α and V β variable region domains and α chain junctional region in viral antigen recognition. *Eur J Immunol* 21: 2195–2202.
6. Schmidt-Supprian M, Rajewsky K (2007) Vagaries of conditional gene targeting. *Nat Immunol* 8:665–668.

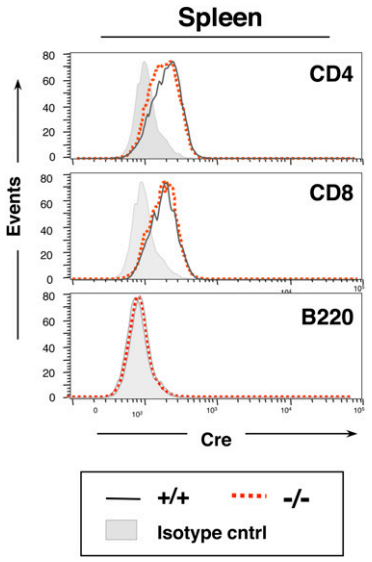

Fig. S1. Lck-driven Cre recombinase expression in Nck.T$^{-/-}$ mice. Targeted Nck deletion to developing and mature T cells was obtained by crossing Nck1$^{-/-}$Nck2$^{flx/flx}$ mice with *Lck*-Cre transgenic mice. Expression of the Cre recombinase was detected in CD4^{+} and CD8^{+} T cells, but not in splenic B cells, as assessed by flow cytometry. Cre expression was comparable in Nck.T$^{-/-}$ (n = 9) and Nck.T$^{+/+}$ (n = 7) mice. Data are representative of five independent experiments.

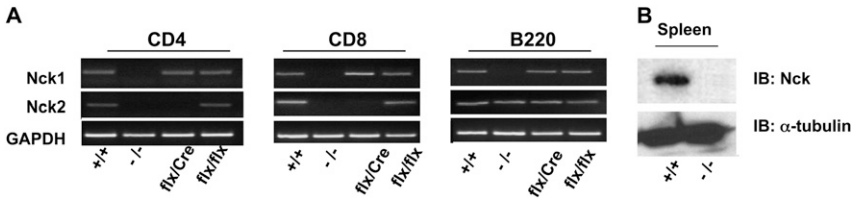

Fig. S2. Efficient Nck deletion in Nck.T$^{-/-}$ mice. (*A*) To assess the deletion efficiency of the *Nck2*.floxed allele, *Nck2* expression was assessed by RT-PCR on different lymphocyte subsets, purified by cell sorting [FACSAria (BD); purity = 97.2 ± 1%] from the spleen of various experimental mouse strains. In brief, total RNA was extracted with the RNeasy kit (Qiagen) and reverse transcribed with the ImProm-II Reverse transcription System kit (Promega), according to the manufacturer's instructions. GAPDH amplification of graded doses of the various cDNA samples was used to quantify and "normalize" their levels, using ImageJ software. After normalization, equal cDNA amounts were amplified using Nck1- and Nck2-specific primers. Cells were derived from Nck.T$^{-/-}$ mice ($^{-/-}$, n = 2) and compared with those from Nck.T$^{+/+}$ ($^{+/+}$, n = 2), *Lck*-Cre Nck1$^{+/+}$ Nck2$^{flx/flx}$ (flx/Cre, n = 2), and Nck1$^{+/+}$ Nck2$^{flx/flx}$ (flx/flx, n = 2) mice. In Nck.T$^{+/+}$ and Nck2$^{flx/flx}$ mice, Nck2 expression was readily detectable. Data are representative of two independent experiments. (*B*) At the protein level, Nck was not detectable in thymic or splenic lysates from Nck.T$^{-/-}$ mice. Data are representative of three separate experiments.

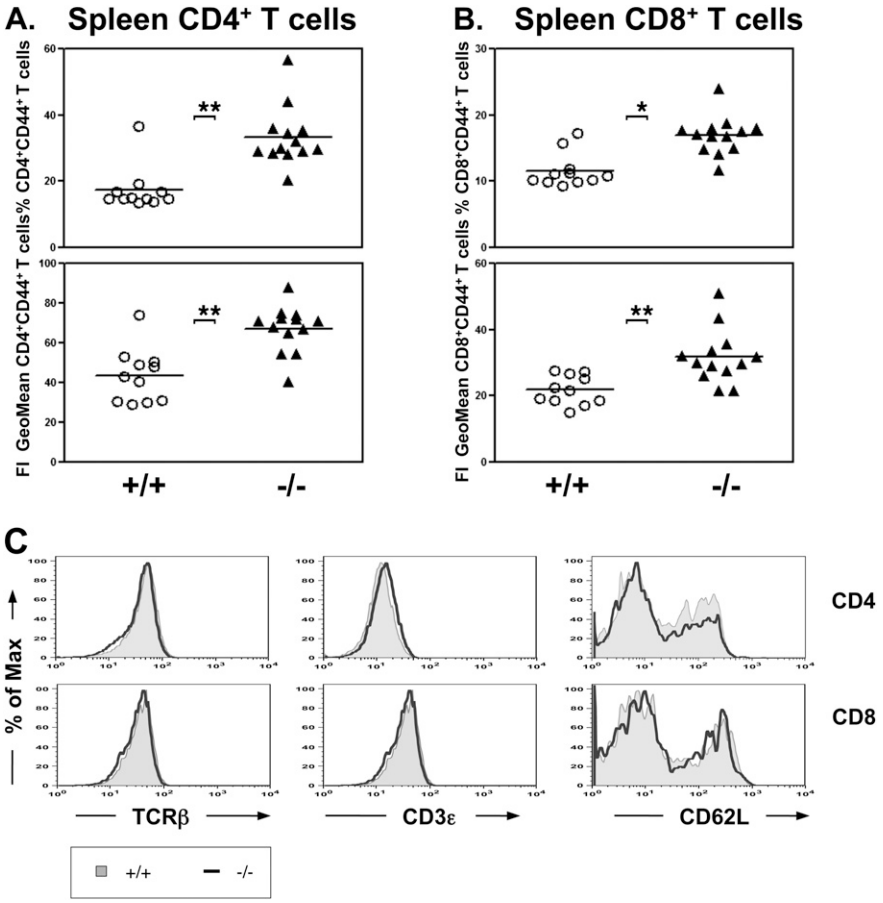

Fig. S3. Increased CD44 expression in Nck-deficient peripheral T cells. The percentage of CD4 (*A*) and CD8 (*B*) T cells expressing CD44 (*Upper*) and the geometric mean of CD44 fluorescence intensity (*Lower*) were assessed by flow cytometry on splenocytes from 5-wk-old, antigen-inexperienced Nck.T$^{+/+}$ (n = 11) and Nck.T$^{-/-}$ (n = 13) mice. The percentage of CD4$^+$CD44$^+$ ($P < 0.0001$) and CD8$^+$CD44$^+$ ($P = 0.0014$), as well as the levels of CD44 expression on CD4$^+$ ($P < 0.0001$) and CD8$^+$ ($P < 0.0001$), T cells were significantly increased in Nck.T$^{-/-}$ mice compared with wild-type controls. Cumulative data from three independent experiments are shown. (*C*) Surface expression of TCRβ, CD3ε, and CD62L on CD4$^+$ and CD8$^+$ splenic T cells from Nck.T$^{-/-}$ (n = 4) and Nck.T$^{+/+}$ (n = 4) mice. Results are representative of at least three independent experiments.

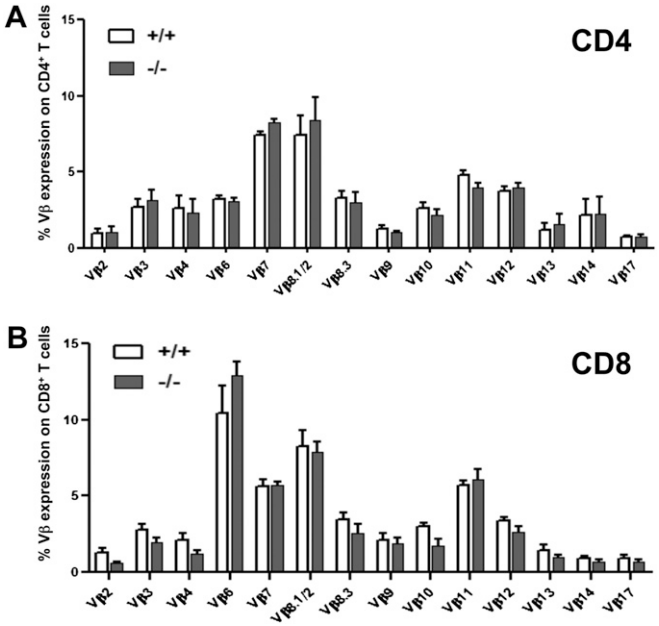

Fig. S4. Comparable Vβ use in the T-cell repertoire of Nck.T$^{+/+}$ and Nck.T$^{-/-}$ mice. To assess the expression of various TCR Vβ chains in the peripheral repertoire, Abs from the Mouse Vβ TCR Screening Panel kit (BD Biosciences) were used in individual sample staining. The percentage of CD4 and CD8 T cells expressing different TCRβ chains was comparable in the spleens of Nck.T$^{+/+}$ (n = 6) and Nck.T$^{-/-}$ (n = 6) mice. Cumulative data (mean ± SEM) from three separate experiments are shown.

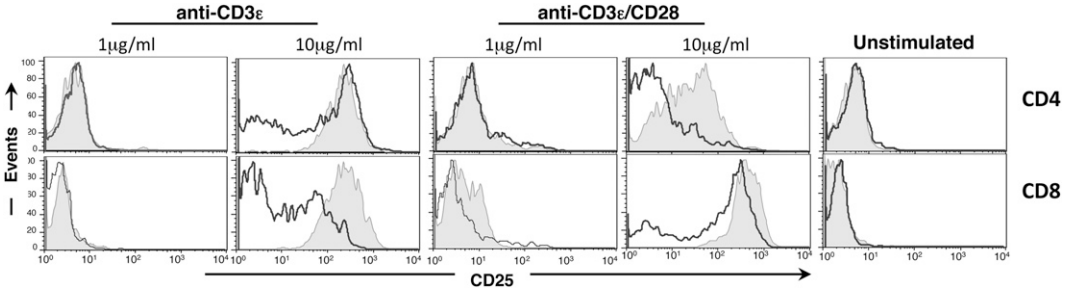

Fig. S5. Reduced IL2R expression in Nck-deficient T-cell cultures. The expression of the high-affinity IL-2 receptor α chain (IL-2Rα; CD25) was assessed on CD4$^+$ and CD8$^+$ T cells isolated from Nck.T$^{-/-}$ (n = 4; line) and Nck.T$^{+/+}$ (n = 4; shaded histograms), upon activation with low (1 μg/mL) and high (10 μg/mL) doses of plate-bound anti-CD3ε or anti-CD3ε/CD28. CD25 expression was markedly reduced in Nck-deficient T cells and only partially rescued by CD28 costimulation.

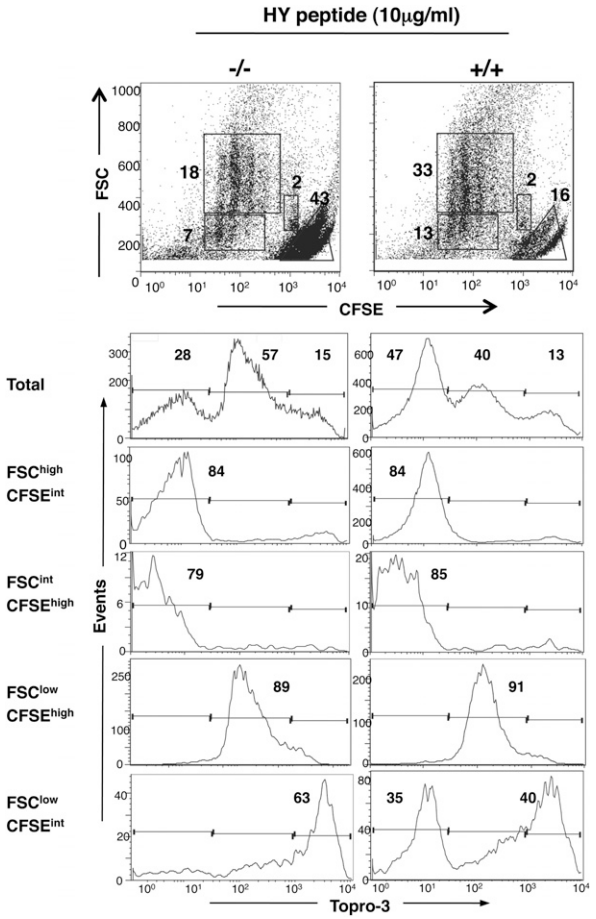

Fig. S6. Reduced viability of in vitro-stimulated Nck-deficient T cells. CFSE-labeled HY-TCR T cells from HY^{RAG}.$NckT^{-/-}$ (n = 3) and $Nck.T^{+/+}$ (n = 5) females were stimulated with D1 dendritic cells loaded with the agonist HY peptide (10 μg/mL). In the CFSE/FSC dot plots, gates delimit clockwise actively proliferating cells ($FSC^{high}CFSE^{int}$), viable nondividing cells ($FSC^{int}CFSE^{high}$), nondividing apoptotic/dead cells ($FSC^{low}CFSE^{high}$), and dividing apoptotic/dead cells ($FSC^{low}CFSE^{int}$). Different levels of Topro-3 staining allow one to define viable (Topro-3^{low}), apoptotic (Topro-3^{dim}), and dead (Topro-3^{high}) cells. Results are representative of two independent experiments.

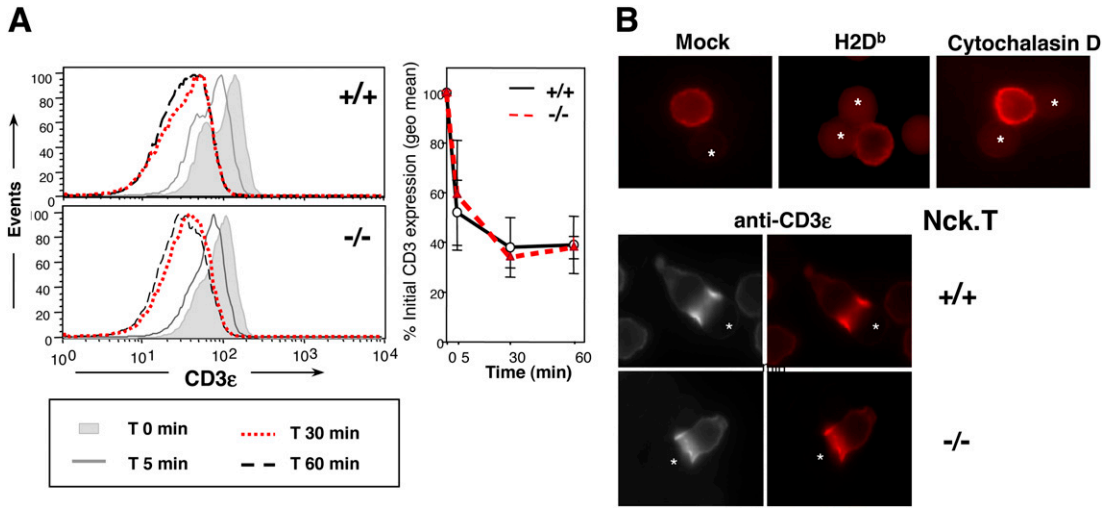

Fig. S7. Nck deletion does not alter TCR internalization and "capping." (*A*) TCR internalization was assessed upon treatment of purified lymph node T cells with α-CD3ε (1 μg/mL, 10 min on ice), followed by cross-linking with biotinylated goat anti-hamster (2 μg/mL, 10 min at 4 °C) and warming up of the cells to 37 °C. The reaction was stopped by fixation with 2% paraformaldehyde at various time points. CD3ε surface levels were quantified by streptavidin-PerCP staining. TCR internalization in Nck.T$^{+/+}$ (n = 3, *Upper*) and Nck.T$^{-/-}$ (n = 3, *Lower*) T cells was assessed 5 min (solid line), 30 min (broken line), and 60 min (dotted line) after CD3ε cross-linking. Shaded histograms represent the CD3ε expression before cross-linking. The graph represents the reduction of CD3ε expression as percentage of the initial CD3ε geometric mean for Nck.T$^{+/+}$ (solid line) and Nck.T$^{-/-}$ (broken line) T cells in three independent experiments. (*B*) For T-cell "capping" experiments, purified T cells were incubated with biotinylated anti-CD3ε (1 μg/mL) or control Ab (10 min on ice), followed by cross-linking with streptavidin-coated magnetic beads (Dynal; 30 min at 37 °C), uncoated beads (Mock), or anti-H-2D^b-coated beads (H-2D^b). Upon fixation with 2% paraformaldehyde, surface staining and intracellular phalloidin staining were performed. Cells were analyzed by fluorescence microscopy. A diffuse ring-like pattern typically appeared upon T-cell interaction with uncoated (Mock), anti-H-2D^b beads or when T cells were pretreated with cytochalasin D. "Capping" induced by CD3ε cross-linking was unaffected by Nck deletion. Results are representative of three separate experiments.

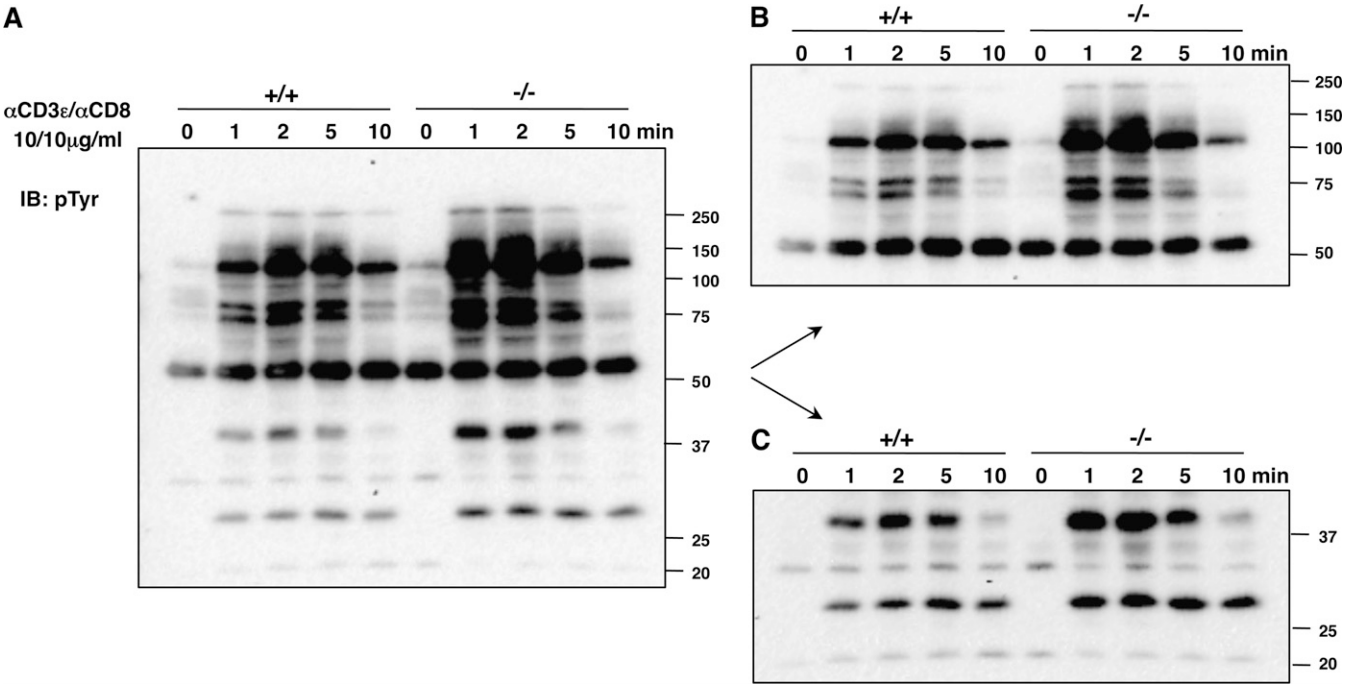

Fig. S8. Tyrosine phosphorylation in Nck.T$^{-/-}$ mice. Freshly isolated thymocytes from Nck.T$^{-/-}$ and Nck.T$^{+/+}$ mice were stimulated by αCD3ε/αCD8 (10 μg/mL) cross-linking and lysed at different time points, as indicated. The induction of tyrosine phosphorylation was assessed by pTyr immunoblotting on total lysates. Because of the differences in signal intensity between high- and low-molecular-weight proteins, different exposures of the same blot are provided in *A* (90 s), *B* (45 s), and *C* (180 s). Data are representative of five independent experiments.

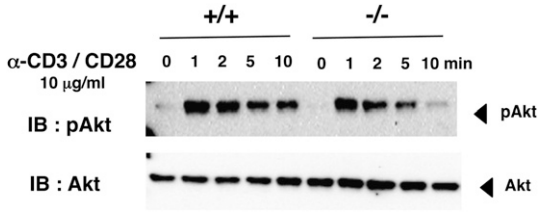

Fig. S9. Akt phosphorylation in Nck.T$^{-/-}$ mice. Freshly isolated thymocytes from Nck.T$^{-/-}$ and Nck.T$^{+/+}$ mice were stimulated by CD3ε/CD8 cross-linking and lysed at different time points. The induction of Akt phosphorylation was comparable in the presence/absence of the Nck adaptors. The levels of Akt phosphorylation underwent a more rapid decline in Nck-deficient thymocytes, but the difference between Nck.T$^{-/-}$ and Nck.T$^{+/+}$ mice did not reach statistical significance (P = 0.0515). Data are representative of three independent experiments.